Pergamon

Journal of Structural Geology, Vol. 20, No. 12, pp. 1663 to 1672, 1998

PII: S0191-8141(98)00053-4

0191-8141/98 $ - see front matter

Thickness and spatial distributions of clastic dykes, northwest Sacramento Valley, California

R. J. H. JOLLY, J. W. COSGROVE and D. N. DEWHURST

T. H. Huxley School of Environment, Earth Science and Engineering, Imperial College of Science, Technology and Medicine, Royal School of Mines, Prince Consort, London, SW7 2BP, U.K.

(*Received* 18 *September* 1997; *accepted in revised form* 28 *May* 1998)

Abstract The geometry and distribution of the clastic dykes of the Ono district, North Sacramento Valley are examined within stream sections. Five traverses along dry stream beds provide good exposure allowing the spacing, thickness and geometry of the dykes to be recorded. The spatial and thickness distribution of the dykes are considered using cumulative frequency plots, allowing a visual estimation of a best fit distribution. Dyke thickness conforms best to a log-normal distribution. There is also a characteristic minimum dyke thickness in a traverse and this is attributed to the minimum aperture that a fluid with sand clasts is able to exploit. Dyke spacing, however, shows a good correlation with a power-law distribution for four traverses, suggesting that there is a mechanistic control on the spatial distribution. Plotting dyke thickness against minimum dyke spacing reveals that thin dykes do not generally intrude in isolation. Unlike veins and igneous dykes, clastic dykes continue to provide preferential pathways for fluid flow, subsequent to their intrusion, thus inhibiting intrusion in the area surrounding a pre-existing dyke. A combination of this process and dyke branching provides the best model for the observed spatial and thickness distribution of clastic dykes seen in the Ono district, California. © 1998 Elsevier Science Ltd. All rights reserved

INTRODUCTION

Clastic dykes occur in a wide range of environments (Maltman, 1994), occurring either as isolated intrusions (Martill and Hudson, 1989), or in swarms (Diller, 1890; Peterson, 1966). Intrusion takes place when there is a rapid loss of fluid from a poorly lithified clastic horizon, resulting in the fluidisation of that horizon (Richardson, 1971; Nichols, 1995). Fluid escapes through the propagation of a fracture; these are normally vertical as typically the minimum compressive principal stress is horizontal. Fluid may also exploit a pre-existing fracture system (Cook and Johnson, 1970; Tuswell, 1972). The sand clasts subsequently infill these fractures resulting in a clastic dyke. The orientations of clastic dykes have been used to infer stress distributions at the time of intrusion (Harms, 1965; Huang, 1988).

One of the first clastic dyke swarms to be recognised was in the northwest Sacramento valley, in the Ono district (Fig. 1), northern California (Diller, 1890). These have been interpreted as a series of intrusions injected along en échelon tension fractures associated with NNE SSW-trending strike-slip faults (Peterson, 1966). They intrude the Budden Canyon Formation, a succession of marine shales, sandstones and conglomerates of Cretaceous age (Murphy *et al.*, 1964). The sands within the clastic dykes are similar to those found within the succession. However, the source horizon for the dykes has not been established and it is therefore difficult to verify the height of the dykes above source.

The intention of this paper is to analyse the range of geometrical forms of clastic intrusions. Spatial and thickness distributions of clastic dykes are also examined and are compared with four distributions, normal, negative-exponential, log-normal, and power-law. The processes that influence the intrusion of clastic dykes are then discussed in the context of dyke thickness, spatial positioning and intrusive form in an attempt to establish those processes that exert the greatest influence in the generation of a clastic dyke swarm.

GEOLOGY OF THE AREA

The Budden Canyon Formation lies unconformably on the Shasta Balley batholith, a quartz–diorite pluton of Late Jurassic age (Kinkle *et al.*, 1956). The Budden Canyon Formation is subdivided into the Rector Conglomerate Member, the Ogo Member, the Roaring River Member, Chickabally Member, Bald Hills Member, and the Gas Point Member (Fig. 1). The members consist of mudstones, sandstones, and conglomerates, the subdivision being based on characteristic sequences of these lithologies (Murphy *et al.*, 1964). The members range in age from Hauterivian to Turonian. Unconformably overlying the Budden Canyon Formation are the Tehama and Red Bluff Formations, of Pliocene and Pleistocene age (Anderson and Russell, 1939).

The Budden Canyon Formation is wedge shaped, thickening from a stratigraphic thickness of 2100 m in the north, to 6700 m in the south. The formation has been folded into an open synform plunging gently

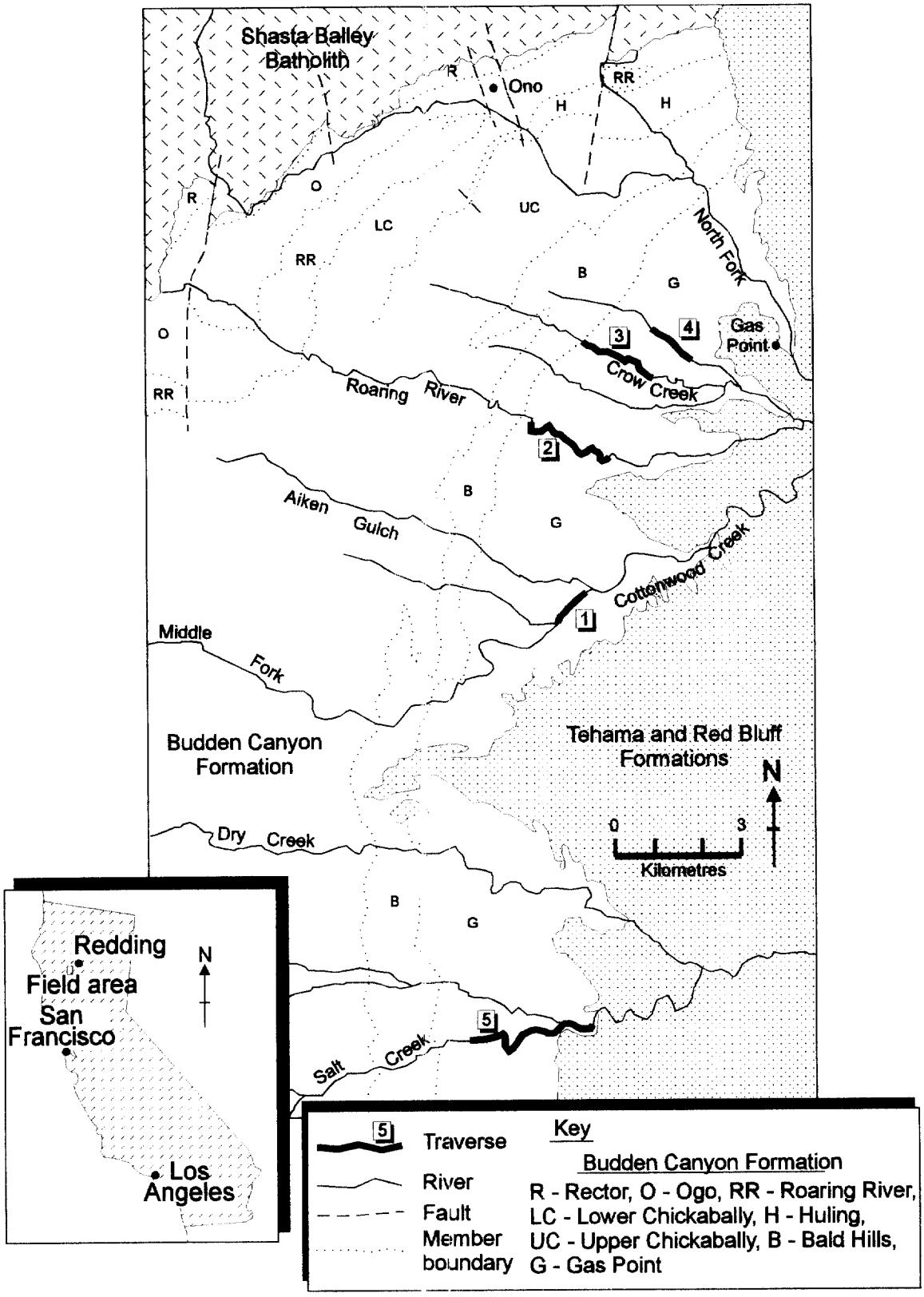

Fig. 1. Geological map of the Ono district (adapted from Peterson, 1966). Indicated on the map are the major streams along which the traverses were measured, the formations, members within the Budden Canyon Formation, and the location of the traverses (numbers in boxes). The map inset shows the position of the field area within California.

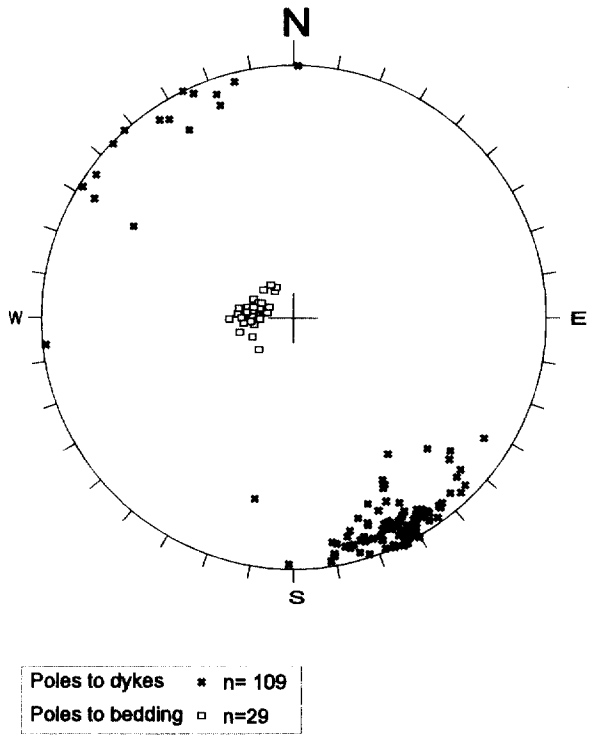

Fig. 2. Equal area stereogram of poles to bedding (solid squares) and the poles to dyke wall (crosses), showing bedding dipping gently to the east, and the consistent dyke trends in approximately the ENE–WSW direction.

towards the east and in the study area the beds typically dip between 10° and 20° to the east (Fig. 2). The clastic dykes are found towards the top of the Budden Canyon Formation, with the majority of dykes cross-cutting the Gas Point Member (Peterson, 1966).

METHODOLOGY

Dry stream beds provide complete exposed sections through the dyke swarm. Traverses were measured in 30 m sections by laying out tapes that were then joined to form the traverse. These record the distance along the traverse of dykes, their thickness, orientation, and geometrical features, such as horn structures and flow textures within the dykes. Streams at a high angle to the mean trend of the swarm were used in order to encounter the maximum possible number of intersections.

Due to the meandering nature of the streams, it was necessary to correct the dyke spacing to 90° to the mean trend of the dykes (see Appendix).

Five traverses were recorded intersecting a total of 77 dykes. The combined corrected length for the traverses is 9070 m. The locations of the traverses can be seen in Fig. 1, and were largely controlled by the exposure of the swarm. As well as the dykes recorded along traverses, the orientations and geometric characteristics of other dykes were noted where poor exposure prevented the use of the traverse technique of collecting data. These dykes, however are not included in the analysis of spacing and thickness.

DYKE ORIENTATION

The clastic dykes intrude the shales perpendicular to bedding (Fig. 2), and show a remarkable degree of alignment (Fig. 2), dip steeply, with 85% dipping to the NNW (Fig. 3a). The dykes typically trend ENE–WSW with a mean strike of 64° (Fig. 3b).

Although the orientations of the dykes are remarkably consistent, there are minor changes in orientation that generate irregularities in dyke form. These manifest themselves in the form of side-steps, branching and merging of the dykes (Fig. 4a & b). Rafts of the host rock are often seen in the dykes, particularly in the thicker dykes (Fig. 4c). These rafts are often found close to an irregularity in the walls of the dykes, suggesting that the formation of wall irregularity and raft is linked.

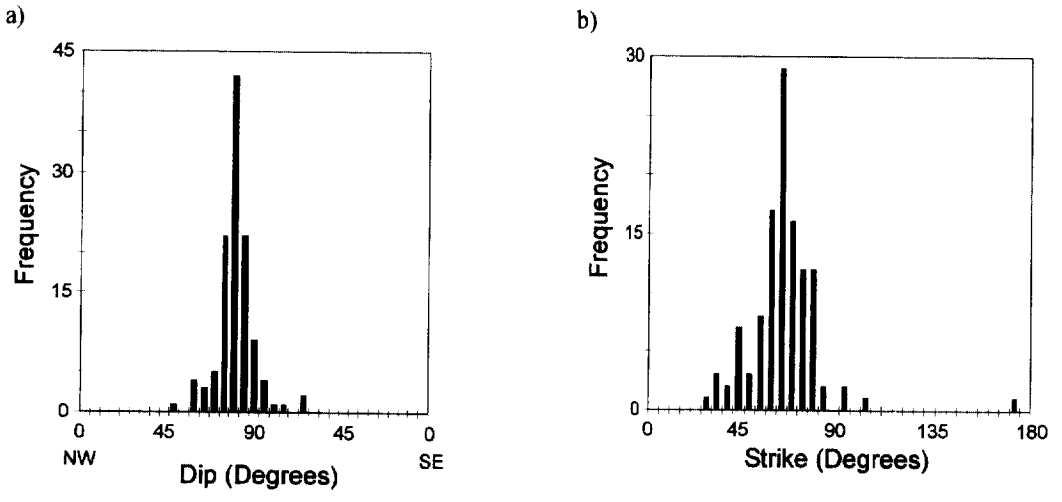

Fig. 3. Frequency histograms of (a) dip and (b) strike of the clastic dykes.

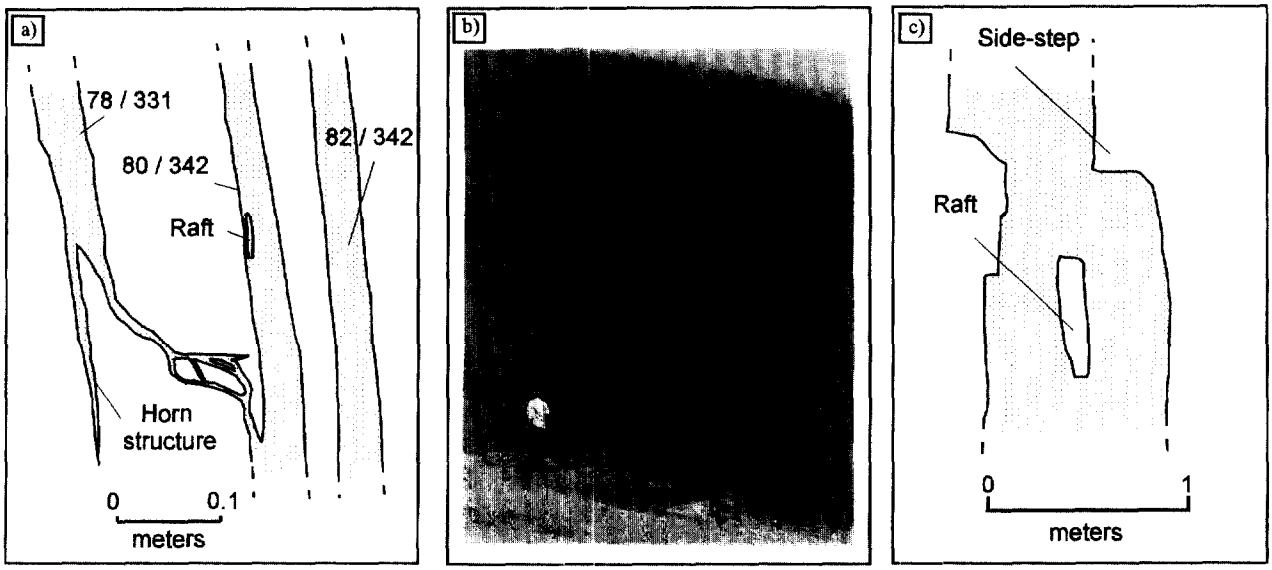

Fig. 4. Maps of the dykes. (a) Thin anastomosing dyke, showing the irregular geometries, and linkage between two of the dykes. (b) Photograph of a planar vertical thick dyke, that is offset along bedding, towards the top. (c) Thicker dyke with a raft of host shale suspended within the intrusion. Rafts are often associated with dyke wall irregularities.

THICKNESS AND SPACING OF THE DYKES

A preliminary glance at the data (Fig. 5) shows that the dykes occur in groups; rarely do they occur in isolation. This is apparent when plotting normalised cumulative thickness against normalised distance (Fig. 5). All the traverses, except traverse 5, have a marked step form (Fig. 5). To examine the nature of the dyke distribution along the traverses, the dyke thickness and spacing distributions were examined separately, and then collectively, so as to establish if there is any influence on each other.

Thickness distributions

The thickness of the dykes, recorded normal to the dyke wall, range from a few millimetres to 1.3 m. The data for each traverse were compared to normal (Gaussian), log-normal, negative-exponential, and power-law distributions using cumulative frequency plots. These plots allow visual evaluation of the data, establishing the correlation between the data and the mathematical distributions. A straight line on one of these plots shows conformity to that distribution.

For traverses 1, 3, 4 and 5 (Fig. 1), there is a good fit to the log-normal distribution (Fig. 6). The data from traverse 2 have the best fit to the negative-exponential distribution (Fig. 6), though none of the model distributions considered completely describe the clastic dyke thickness data for this traverse. The clastic dyke thickness data clearly do not correspond to a power-law distribution, unlike other fracturing phenomena such as vein thickness (Sanderson *et al.*, 1994; Manning, 1994; Johnston and McCaffrey, 1996), fault displacement (Walsh *et al.*, 1991; Peacock and Sanderson, 1994), and fracture aperture (Barton and Zoback, 1992). It can be seen that, when displayed on the power-law plots (Fig. 6), the data show a characteristic tailing-off for dykes less than 0.1 m. As dykes of this size would have been easily observed using the traverse method, it is clear that the observed tail-off of the data is real and not an artefact of the sampling truncation caused by failing to record dykes with thickness of less than 0.1 m.

The formation of igneous dykes provides another example of a fracturing process that does not conform

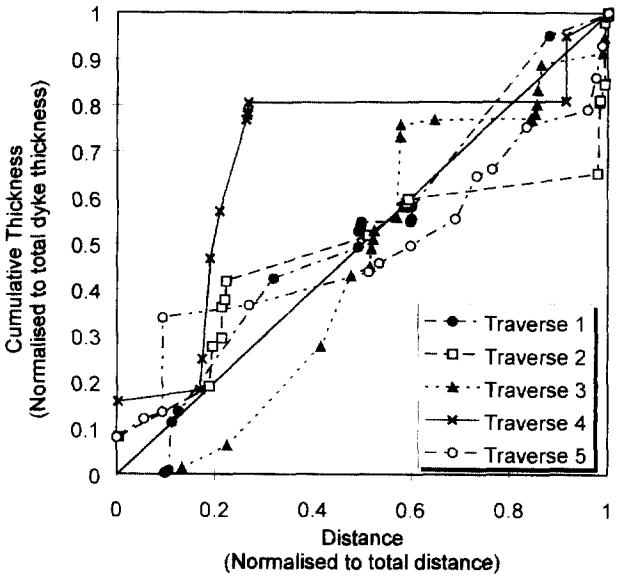

Fig. 5. Cumulative thickness of the clastic dykes, normalised to total thickness, plotted against their distance along the traverse, normalised to the total traverse length, for all five traverses. The distinctive stepped form of the plots shows the spatial grouping of the dykes measured along the traverses. The diagonal line shows the line along which an even spatial and thickness distribution would plot.

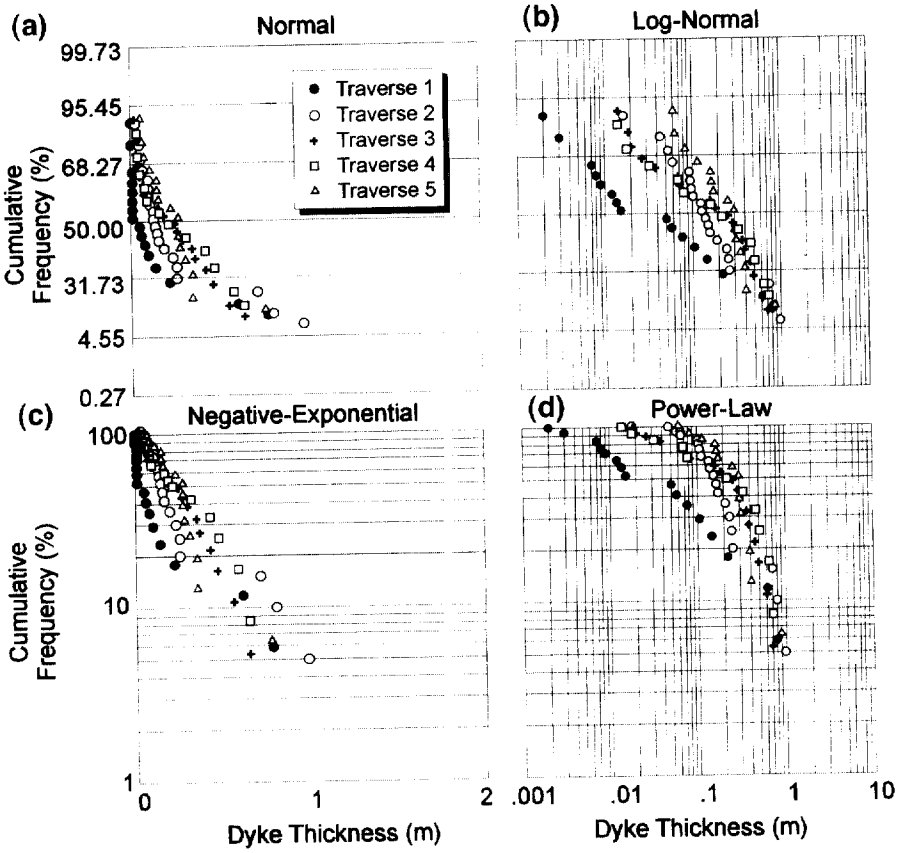

Fig. 6. The thickness data plotted on cumulative frequency graphs, allowing a visual comparison with (a) normal (Gaussian), (b) log-normal, (c) negative-exponential, and (d) power-law distributions. A straight line on one of these plots indicates a good correlation between the data and that distribution, for example traverse 1 (a) has a good correlation with a power-law distribution.

to a power-law distribution (Jolly and Sanderson, 1995). The displacement (dilation) associated with their intrusion is found to have a log-normal distribution. The deviation from the power-law model, in this case, can be attributed to the scale limiting process of freezing, preferentially removing thin dykes from the distribution (Jolly, 1996). Although freezing is not applicable to clastic dykes a similar process is proposed in the discussion section of this paper to explain this deviation from the power-law model.

Spacing distributions

Dyke spacing along the traverses was measured between the centres of adjacent dykes. This spacing was then corrected so that the spacing normal to mean dyke trend for each traverse was used in the distribution analysis (see Appendix). Once the spacing correction had been applied to the data, it was treated in the same way as the thickness data from the traverses. The corrected spacing was again compared to normal, log-normal, negative-exponential and power-law distributions. A straight line in one of these plots indicates a conformity to that distribution. For all of the traverses, except traverse 5, the corrected dyke spacing shows the best conformity to either power-law or log-normal distributions (Fig. 7). The fact that these traverses do not conform to a negative-exponential distribution, and are not random, suggests that there is an organisational control on the spatial position of the dykes. Traverse 5 has the best conformity to a negative-exponential distribution (Fig. 7). The line sampling method, however imposes a scale limit truncation to the data, where there is a low probability of intercepting spaces above a certain size within a finite distance. This has the effect of causing a tail-off on the power-law cumulative frequency plots (Pickering *et al.*, 1995). The data show good conformity to a power-law distribution for 2.5 orders of magnitude, and where the size of the spaces approaches within two orders of magnitude of the total length of the traverse, the data deviate away from the power-law distribution. The tail-off at the upper limit of dyke spacing is almost certainly the result of sampling, i.e. there is a low probability of having spaces between dykes greater than 100 m, when the total traverse lengths are typically less than 1500 m. As this tail-off can be attributed to a sampling effect on the data, it is felt that the data shows closest conformity to a power-law distribution. This is perhaps seen more clearly when the spacing data are plotted against cumulative frequency per metre (Fig. 8).

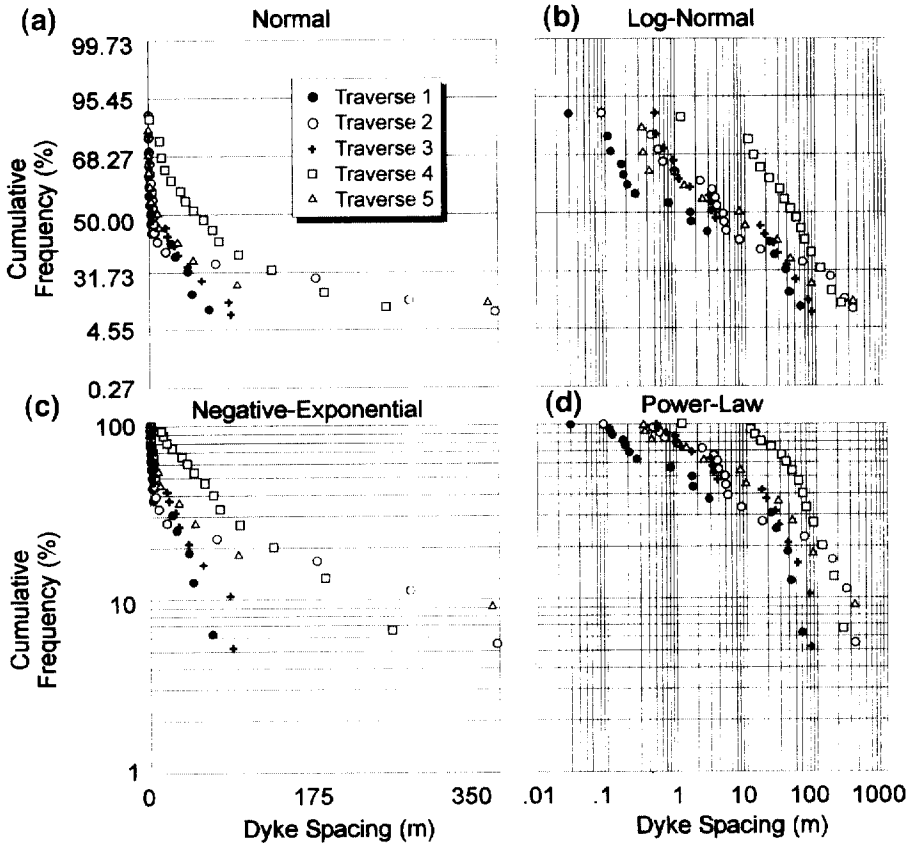

Fig. 7. The spacing data plotted on cumulative frequency graphs, allowing a visual comparison with (a) normal (Gaussian), (b) log-normal, (c) negative-exponential, and (d) power-law distributions. A straight line on one of these plots show a good correlation between the data and that distribution, for example traverse 1 has a good correlation with a power-law distribution.

Plotting dyke spacing against cumulative frequency per metre allows a comparison of the distributions along the five traverses to be examined (Fig. 8). For the first four traverses the data have a similar gradient (Fig. 8). The dimension of these power-law distributions, which is found from the gradient of the distribution, ranges from 0.25 to 0.33 (Fig. 8). A power-law distribution suggests that the system is scale-invariant, at least over 2.5 orders of magnitude, and therefore exhibits fractal behaviour. Pickering *et al.* (1995) express the power-law relationship in terms of the cumulative number (N), a constant (a), a measure of size (u), in this case spacing, and the exponent b, the dimension of the distribution [equation (1)].

$$N = au^{-b} \tag{1}$$

Using the gradients from the cumulative distribution plots, a dimension of 0.29 is obtained for the spacing of the dykes. The Cantor–Dust model (Mandelbrot, 1983) has been used to demonstrate the fractal nature of mode I extensional fractures (Velde *et al.*, 1990; Kruhl, 1994) and is a useful aid in visualising the meaning of a fractal dimension. This model is a one dimensional fractal relationship, and simply involves dividing a bar into segments (Fig. 9) and removing one or more segments. This process is then repeated, dividing each remaining segment into the same number of segments, and removing one or more of those segments (Fig. 9). A low dimension, much less than 1

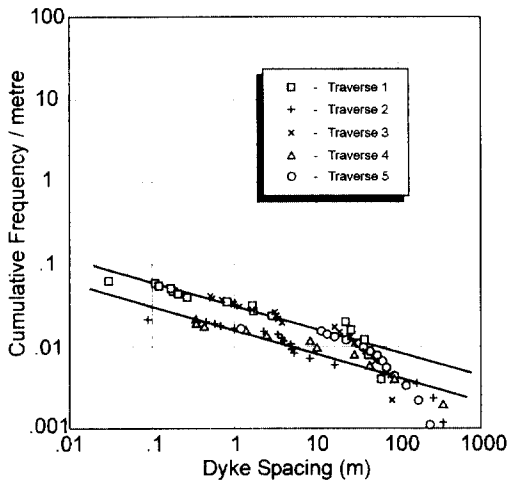

Fig. 8. Log of dyke spacing plotted against log cumulative frequency per metre for comparison of the gradients of the power-law distribution for all five traverses. As can be seen from the plot they yield similar gradients, of approximately 0.29, except for traverse 5. The two lines shown have gradients of 0.29, and are given as a reference lines against which to compare the slopes of the different data sets.

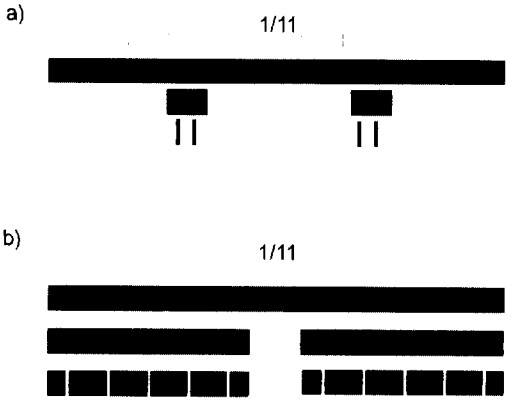

Fig. 9. The Cantor–Dust model is a one dimensional fractal algorithm. Two variations of the algorithm are presented here. (a) where the dimension is 0.29, and (b) where the dimension is 0.96. A bar is divided up into segments, some of which are removed, in the case of (a), and nine, in the case of (b). This process is then repeated, dividing the remaining segments into 11 segments, and removing one segment, in the case of (a) or nine, in the case of (b), this process then repeated again. A low dimension, much less than 1, suggests that large spaces are found in abundance relative to small spaces, the dykes are, therefore, very localised (a). A higher dimension, closer to 1, suggests that small spaces dominate relative to large spaces and that dykes are much more space filling (b).

(such as 0.29, as obtained from the spacing distribution in Fig. 8), suggests that large spaces are found in abundance relative to small spaces and the dykes are, therefore, very localised (Fig. 9a). A higher dimension, closer to 1, suggesting that small spaces dominate relative to large spaces, means that dykes are much more space filling (Fig. 9b). Clearly, a dimension of 0.29 shows that the clastic dykes are extremely clustered, forming intrusive pockets within the shales, similar to the Cantor–Dust distribution (Fig. 9a). The consistency of the dimension for clastic dyke spacing implies that there is some controlling factor for the spatial distribution of the Ono dyke swarm.

Thickness–spacing relationship

The plotting of spacing against thickness allows the examination of the relationship of these two variables. The spacing (S) is calculated using the distances, from the centre of the dyke to the centre of the nearest dykes on either side, before (l_b) and after (l_a) along the traverse.

$$S = \frac{l_b + l_a}{2} \qquad (2)$$

There is little correlation between spacing and thickness, though the dykes with the smallest spacing are also the thinnest dykes (Fig. 10a). The data, however, show a large scatter, and have no obvious trend. This method of examining the correlation between spacing and thickness, however, often obscures close spatial relationships, as a result of combining small distances, less than 1 m, with large distances, greater than 100 m, thus hiding the true influence of an adjacent dyke. A better method is to plot the minimum distance to an adjacent dyke against thickness. This shows the influence of dyke thickness on the spacing of adjacent dykes. Using this approach a better correlation between dyke thickness and the spatial position of adjacent dykes is found (Fig. 10b).

Thin dykes are not able to intrude in isolation, thus they do not have a large minimum spacing (Fig. 10b). A thick dyke can have a small minimum spacing (Fig. 10b), though these are often due to an associated thin dyke, and rarely are two thick dykes seen adjacent to each other. The thin dykes associated with a thick dyke could be horn structures (Fig. 4a), or may have branched from the thick dyke.

DISCUSSION

The high degree of alignment of the dykes suggests that they were intruded into a stress system where the intermediate compressive stress was much greater than

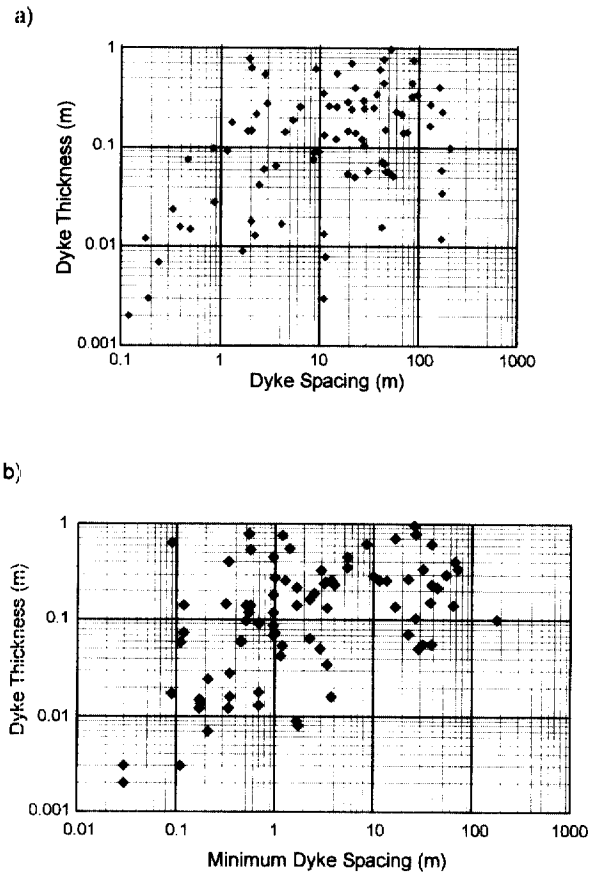

Fig. 10. (a) Dyke thickness plotted against dyke spacing, where dyke spacing is half the total spacing between the two adjacent dykes. As can be seen from the plot there is no significant correlation between the thickness and spacing of these dykes. (b) Dyke thickness plotted against minimum dyke spacing, the minimum distance to an adjacent dyke. Here there is a better correlation: more importantly there is a cut-off at the lower right hand side which shows that thin dykes are not discrete. This indicates that these clastic dykes are sensitive to each other.

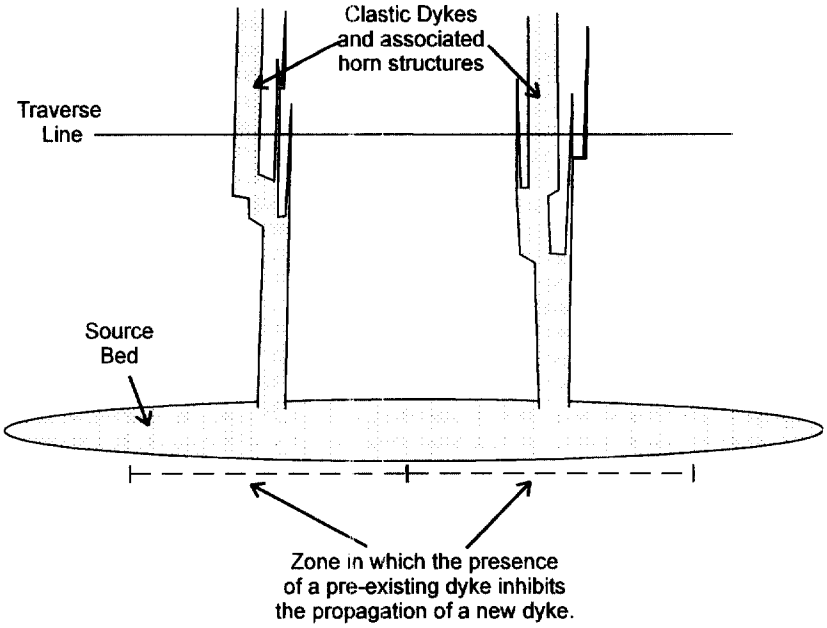

Fig. 11. Schematic model for the clastic dykes, showing the influences of the processes of branching and dyke sensitivity on the spatial and thickness distributions seen in the Budden Canyon Formation. The connectivity of the dykes through the source beds inhibits the intrusion of dykes adjacent to pre-existing dykes. Branching, side-stepping and the formation of horn structures causes there to be a spatial clustering of the dyke at a higher level in the sequence, as is reflected in the spatial data.

the minimum compressive stress. Dykes intruding into a system with the intermediate and minimum compressive stress equal will have a wide range of orientations and therefore link (Renshaw and Pollard, 1994). This suggests that there was a tectonic influence at the time of intrusion of these dykes (Peterson, 1966).

The dyke thickness distributions for four out of the five traverses are log-normal (Fig. 6). Therefore, unlike veins and faults, clastic dykes do not have a fractal distribution for their displacement (dilation). The dykes also have a distinct range of thicknesses, from approximately 0.01 to 1 m. Where there are some thinner dykes, as in traverse 1, they form small clusters of linked dykes that have a combined thickness of 0.09 m. This suggests that there is a minimum thickness for an intruding dyke, and explains why clastic dyke thickness distribution does not conform to the fractal model. A possible explanation for such a lower limit to dyke thickness, is that a minimum aperture is necessary before clasts can be carried along with the flow of the expelled pore fluid (Kern *et al.*, 1959; Perkins and Kern, 1961). This imposes a scale limiting process on the dilation of a fracture, and explains why clastic dykes do not conform to a fractal distribution.

The low dimension, 0.29, for dyke spacing implies that the intrusion of these dykes is extremely clustered. The exceptional localisation of the clastic intrusions could reflect a number of mechanisms:

(a) The localisation could be the result of the spatial positioning of the source pockets of sand within the Budden Canyon Formation, and thus the spatial relationship of these dykes reflects the distribution of the source sand pockets.
(b) Repeated branching of thin clastic dykes from a main dyke will produce a spatial clustering of intrusions (Fig. 11). Thick dykes, greater than 1 m, often have thin dykes associated with them. The branching of dykes typically occurs where the dyke has side-stepped, as illustrated in Fig. 11.
(c) The spatial relationship of the dykes could be controlled by the spatial distribution of stress associated with tectonic deformation. With this mechanism however, a clustering of the dykes in the zone of most intense deformation should be seen. Although the dykes do show an intense clustering it is difficult to link them to a particular structure. However, as mentioned earlier, the high degree of alignment of the dykes does suggest that the orientation of these dykes is controlled by a tectonic stress field.

The relationship between dyke thickness and minimum dyke spacing shown in Fig. 10(b), indicates that dykes are sensitive to the presence of adjacent dykes, and therefore influence the locations of sites of subsequent intrusion. It is suggested that unlike other fracture flow phenomena in the crust, such as veins and igneous dykes, which after mineralisation or magma solidification no longer act as permeable pathways, clastic dykes, once formed, continue to provide favourable flow pathways, as the sand within the fracture is more permeable than the shales into which it has intruded. This therefore facilitates a drop in fluid

pressure in the sediments immediately adjacent to a dyke and thus inhibits the formation of new dykes in these areas. Clearly this process would hinder the clustering of thick dykes.

The spatial relationship is probably the result of more than one of these processes, as any one of them in isolation will not produce the spatial and thickness distribution seen in the clastic dykes of the Budden Canyon Formation. Branching of dykes is a commonly observed phenomena within the clastic dykes of the Budden Canyon Formation. This, in combination with the sensitivity of dykes to each other, is probably the most likely explanation for the development of the observed intrusive spatial arrangement (Fig. 11). The dykes are spatially organised at the point of intrusion from the source bed, as they are sensitive to the positions of the adjacent clastic intrusions (Fig. 11). Irregularities in the dyke walls during intrusion into the shales cause the dykes to branch forming local clusters of intrusions (Fig. 11).

CONCLUSIONS

(a) Dyke thickness distribution shows conformity to a log-normal distribution, suggesting a scale limiting process affecting clastic dyke thickness. This is attributed to a minimum aperture required for intrusion, controlled by the grain size of the sand within the fluid.
(b) Spacing generally has a good conformity to a power-law distribution. The fractal dimensions are also consistent at approximately 0.29. This suggests that clastic dyke intrusion is extremely localised.
(c) There is a correlation between dyke thickness and minimum dyke spacing implying that dykes are sensitive to the presence of adjacent dykes. This may reflect the fact that they remain preferential flow pathways through low permeability sediments.
(d) It is suggested that the most likely mechanism for generating the thickness and spatial distribution of these dykes is a combination of dyke branching and the sensitivity of the dykes to each other.

Acknowledgements—This work was funded by two NERC Ropa awards (RJHJ/DD). Thanks to Gary Peterson for guiding us in the direction of this dyke swarm. Thanks also to Dave Sanderson, Lidia Lonergan and Joe Cartwright for their help and discussions about the data. Ken McCaffrey and an anonymous reviewer are thanked for their helpful comments on revising the manuscript.

REFERENCES

Anderson, C. A. and Russell, R. D. (1939) Tertiary formations of northern Sacramento Valley, California. *California Journal of Mines and Geology* **35**, 219–253.

Barton, C. A. and Zoback, M. (1992) Self similar distribution and properties of macroscopic fractures at depth in crystalline rock Cajon Pass scientific borehole. *Journal of Geophysical Research* **97**, 5181–5200.

Cook, A. C. and Johnson, K. R. (1970) Early joint formation in sediments. *Geological Magazine* **110**, 361–368.

Diller, J. S. (1890) Sandstone dikes. *Geological Society of America Bulletin* **1**, 411–442.

Harms, J. C. (1965) Sandstone dikes in relation to Laramide faults and stress distribution in the Southern Front Range, Colorado. *Geological Society of America Bulletin* **76**, 981–1002.

Huang, Q. (1988) Geometry and tectonic significance of Albian sedimentary dykes in the Sisteron area, SE France. *Journal of Structural Geology* **10**, 453–462.

Johnston, J. D. and McCaffrey, K. J. W. (1996) Fractal geometries of vein systems and the variation of scaling relationships with mechanism. *Journal of Structural Geology* **18**, 349–358.

Jolly, R. J. H. and Sanderson, D. J. (1995) The variation in the form and distribution of dykes in the Mull swarm, Scotland. *Journal of Structural Geology* **17**, 1543–1557.

Jolly, R. J. H. (1996) Mechanisms of igneous sheet intrusion. Ph.D. thesis, University of Southampton.

Kern, L. R., Perkins, T. K. and Wyant, R. E. (1959) The mechanics of sand movement in fracturing. *Transactions of the American Institute of Mining Engineers* **216**, 403.

Kinkle, A. R., Hall, W. E. and Albers, J. P. (1956) Geology and base metal deposits of West Shasta copper zinc district, Shasta County, California. *U.S. Geological Survey Professional Paper* **285**.

Kruhl, J. H. (1994) The formation of extensional veins: an application of the Cantor Dust model. In *Fractals and Dynamic Systems in Geoscience*, ed. J. H. Kruhl, pp. 95–104. Spinger-Verlag, Berlin.

Mahman, A. (1994) *The Geological Deformation of Sediments*. Chapman & Hall, London.

Mandelbrot, B. B. (1983) *The Fractal Geometry of Nature*. Freeman, New York.

Manning, C. E. (1994) Fractal clustering of metamorphic veins. *Geology* **22**, 335–338.

Martill, D. M. and Hudson, J. D. (1989) Injection clastic dykes in the Lower Oxford Clay (Jurassic) of Central England—Relationship to compaction and concretion formation. *Sedimentology* **36**, 1127–1133.

Murphy, M. A., Peterson, G. L. and Rodda, P. U. (1964) Revision of Cretaceous lithostratigraphic nomenclature Northwest Sacramento Valley, California. *Bulletin of the American Association of Petroleum Geologists* **48**, 496–502.

Nichols, R. J. (1995) The liquification and remobilization of sandy sediments. In *Characterisation of Deep Marine Clastic Systems*, eds A. J. Hartley and D. J. Prosser, pp. 63–76. Geological Society Special Publication, **94**.

Peacock, D. C. P. and Sanderson, D. J. (1994) Strain and scaling of faults in the chalk at Flamborough Head, UK. *Journal of Structural Geology* **16**, 97–107.

Perkins, T. K. and Kern, L. R. (1961) Widths of hydraulic fractures. *Journal of Petroleum Geology* **13**, 937–949.

Peterson, G. L. (1966) Structural interpretation of sandstone dikes, Northwest Sacramento Valley, California. *Geological Society of America Bulletin* **77**, 833–842.

Pickering, G., Bull, J. M. and Sanderson, D. J. (1995) Sampling power-law distributions. *Tectonophysics* **248**, 1–20.

Renshaw, C. E. and Pollard, D. D. (1994) Are differential stresses required for straight fracture propagation paths? *Journal of Structural Geology* **16**, 817–822.

Richardson, J. F. (1971) Incipient fluidization and particulate systems. In *Fluidization*, eds J. F. Davidson and D. Harrison, pp. 25–64. Academic Press, London.

Sanderson, D. J., Roberts, S. and Gumiel, P. (1994) A fractal relationship between vein thickness and gold grade in drill core from the La Cordosera, Spain. *Economic Geology* **89**, 168–173.

Truswell, J. F. (1972) Sandstone sheets and related intrusions from Coffee Bay, South Africa. *Journal of Sedimentary Petrology* **42**, 578–583.

Velde, B., Dubois, J., Touchard, G. and Badri, A. (1990) Fractal analysis of fractures in rocks the Cantor Dust method. *Tectonophysics* **179**, 345–352.

Walsh, J. N., Watterson, J. and Yielding, G. (1991) The importance of small-scale faulting in regional extension. *Nature* **351**, 391–393.

APPENDIX

Notation

x_o, y_o The x and y co-ordinates of the start of the traverse.
x_n, y_n The x and y co-ordinates of the dyke.
D_t The total distance along the traverse to the dyke.
D_c The corrected distance to the dyke.
D_s Segment length.
μ_n The direction from the dyke to the start of the traverse.
α_n The strike of a segment.
β_n The strike of the dyke.

The methodology used to correct for dyke spacing is outlined below (Fig. 12). The first stage is to establish the location of the dyke relative to the start of the traverse, here we use the length of each segment (D_s) and the strike of each segment (α_n) (Fig. 12).

$$x_n - x_o = \sum_{1}^{n} (D_s \cos \alpha_n) \tag{A1}$$

$$y_n - y_o = \sum_{1}^{n} (D_s \sin \alpha_n) \tag{A2}$$

Having established the location it is possible to find the direction from the dyke to the start of the traverse (μ_n) (Fig. 12).

$$\mu_n = \tan^{-1}\left(\frac{x_n - x_o}{y_n - y_o}\right) \tag{A3}$$

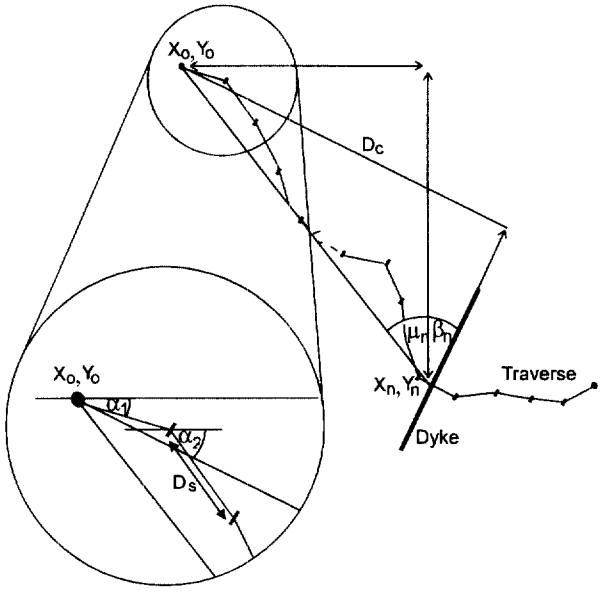

Fig. 12. A schematic diagram showing the notation used to find the corrected spacing of dykes from an anastomosing traverse; details of the methodology can be seen in the text.

Using this angle (μ_n) and the strike of the dyke (β_n), the corrected spacing (D_c) can be found (Fig. 12).

$$D_c = \sqrt{(x_n - x_o)^2 + (y_n - y_o)^2} \sin(\mu_n - \beta_n) \tag{A4}$$